

25 Gbaud DQPSK Receiver Integrated on the Hybrid Silicon Platform

Stefano Faralli^{1,2}, Kimchau N. Nguyen¹, Hui-Wen Chen¹, Jon D. Peters¹, John M. Garcia¹, Daniel J. Blumenthal¹, John E. Bowers¹

1. Electrical and Computer Engineering Department, University of California, Santa Barbara CA 93106

2. Scuola Superiore Sant'Anna, 56124 Pisa, Italy

Author e-mail address: stefano@ece.ucsb.edu

Abstract: A monolithic 25 Gbaud DQPSK receiver based on delay interferometers and balanced detection was fabricated on hybrid silicon platform. We report preliminary results regarding the characterization of the InGaAs p-i-n photodetectors and the delay interferometer.

OCIS codes: (060.4510) Optical communications; (060.5060) Phase Modulation; (130.6750) Integrated Optics-Systems

1. Introduction

Phase modulated formats have attracted attention in the last few years for next generation optical communication systems [1]. In particular, the multilevel modulation and detection techniques naturally enable high bit rate optical transmission such as 40 G SONET and 100 G Ethernet. Differential Quadrature phase-shift keying (DQPSK) has received great attention because it doubles the spectral efficiency compared with the binary formats and different solutions have recently been proposed enabling this technology for in-field optical transmission systems [2]. The conventional method for the demodulation of the DQPSK optical signal consists of a demodulator that converts optical phase modulation into intensity modulation, and in particular consists of two Mach-Zehnder delay interferometers for demodulation of both the signal quadratures, followed by balanced photodetectors. The interferometers have a delay of one symbol period and a different phase-shifts ($\pm\pi/4$) for correct detection of the different signal quadratures; due to their differential detection scheme, this detection does not require a low linewidth laser or high speed signal processing for carrier phase estimation and the DQPSK receivers on silicon are of interest for their potential compatibility with low cost, high volume and mature CMOS processes [3-4]. In this paper we report the design of the integrated DQPSK receiver fabricated on the hybrid Silicon platform [5] and the characterization of the delay interferometers and balanced photodetectors integrated in a single PIC.

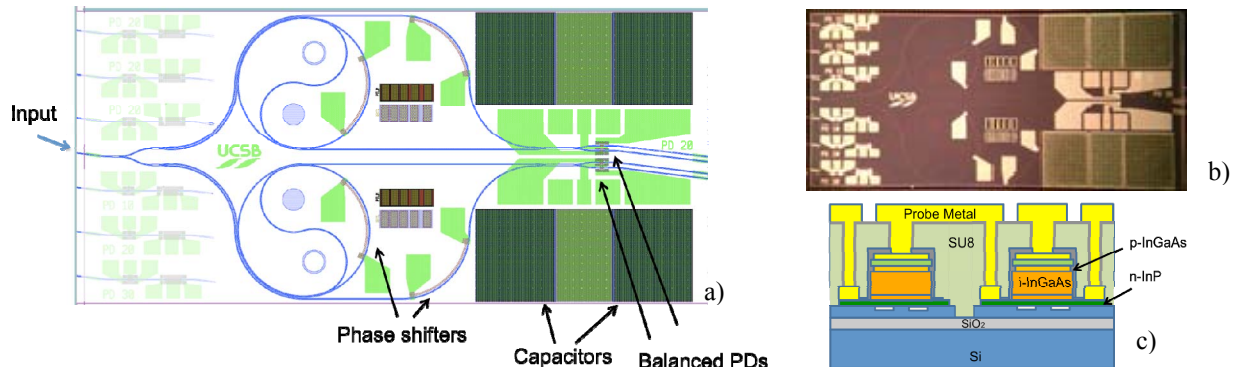


Fig. 1 Mask layout of the DQPSK receiver based on Mach-Zehnder delay interferometers (a). Waveguides are shown in blue, metal contacts are light green. The layout includes stand-alone single PD test structures on the left. Photograph of the receiver PIC (b) and details of the balanced p-i-n InGaAs PD structure (c).

The DQPSK receiver consists of two multimode (MMI) based couplers and 40 ps delay interferometers with four NiCr heater phase shifters, two balanced InGaAs p-i-n photodetector pairs, and four on-chip MIS (metal-insulator-semiconductor) capacitors (Fig. 1). The two interferometers are biased at $\pi/4$ and $-\pi/4$ in order to receive the different signal quadratures. The waveguide structure is SOI with a 0.7 μm waveguide height and 0.3 μm etch depth. The phase shifters are NiCr heaters 10 μm wide and 500 μm long.

2. Photodetector Design and Characterization

The balanced photodetectors shown in Fig. 1 have a similar structure as the single photodetector reported in [6]. The PD performance was evaluated and designed in terms of frequency response and responsivity. The simulated 3-dB bandwidth vs. the intrinsic layer thickness is shown in Fig. 2a and takes into account both the RC and transit-time

limitations. Since the thickness of the intrinsic layer affects the RC and transit-time characteristics in opposite ways, the optimum thickness for the bandwidth can be found in the thickness range of $0.25 - 0.5 \mu\text{m}$, depending on the PD length. The shortest PD of $10 \mu\text{m}$ is expected to have the largest bandwidth of over 50 GHz for an intrinsic thickness of about $0.35 \mu\text{m}$. The expected quantum efficiency of PDs of different lengths is plotted in Fig. 2b assuming a $0.5 \mu\text{m}$ intrinsic layer thickness. As shown, PDs with a length of up to $30 \mu\text{m}$ have a bandwidth over 25 GHz and the (normalized) quantum efficiency is close to 1 for PD lengths down to $10 \mu\text{m}$. The photodiode for the required bandwidth and efficiency at 25 Gb/s operation was fabricated with a length of $30 \mu\text{m}$ and a $0.5 \mu\text{m}$ thick intrinsic InGaAs absorber region. Single PIN photodetectors have been fabricated on the hybrid silicon platform and p-InGaAs, intrinsic InGaAs and n-InP are the p contact layer, intrinsic layer, n contact layer, respectively. The detailed epitaxial layerstack used for fabrication is reported in [6], with the modification of a superlattice to minimize the propagation of defects from the bonded layer to the i-InGaAs layer during the silicon to III/V wafer bonding process. This in turn should minimize the dark current of the PD.

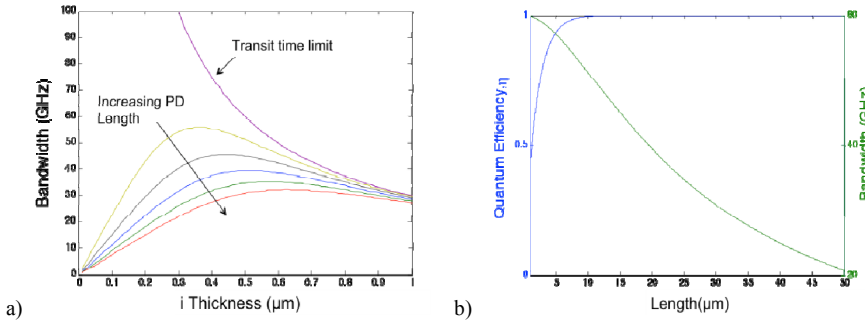


Fig.2 a) Simulated 3-dB bandwidth as a function of intrinsic absorption layer thickness. PD lengths shown are $10, 15, 20, 25$ and $30 \mu\text{m}$. b) Simulated quantum efficiency and bandwidth as a function of PD length assuming a $0.5 \mu\text{m}$ intrinsic layer thickness

Preliminary photodetector (PD) characterization, in terms of frequency response and receiver sensitivity, was done on stand-alone single photodetector test structures fabricated with the receivers. The 3 dB bandwidth of the PD has been measured using a lightwave component analyzer (LCA). The LCA includes an optical modulated source at 1550 nm and an RF probe that collects the RF signal generated by the PD. A bias tee is used to set the PD bias voltage and the RF signal is sent to the lightwave analyzer through the bias tee. The optical signal is coupled into the input waveguide of the photodetector by a lensed fiber with a focused spot size of $3.3 \mu\text{m}$ and the estimated coupling loss is $\sim 8 \text{ dB}$. Figure 2 a) shows the 3dB bandwidth measurements for a $30 \mu\text{m}$ PIN photodetector at different bias voltages. As expected the bandwidth of the photodetector increases as the reverse bias voltage increases due to the increase in carrier velocity. For a 3 V reverse bias voltage, the PDs have a 3 dB bandwidth larger than 25 GHz .

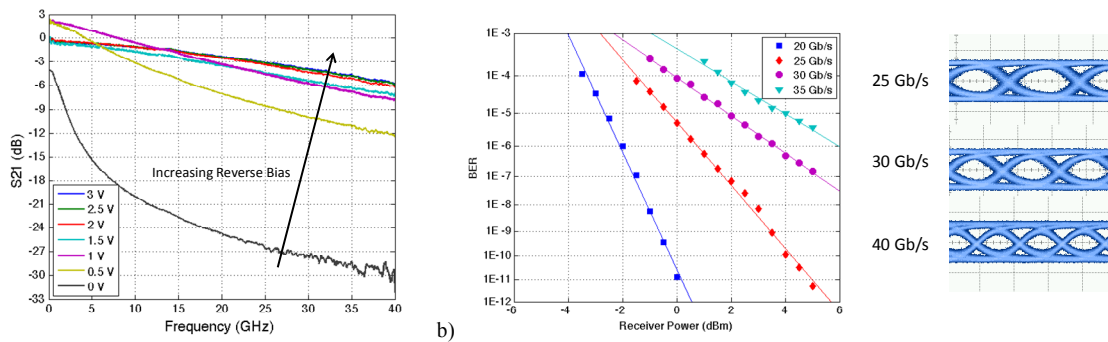


Fig.3 a) Frequency response at different reversed bias voltages for a $30 \mu\text{m}$ long Photodiode b)Measured Bit Error Rate versus received optical power assuming a coupling loss of 8 dB and corresponding Eye Diagram for different modulation frequencies for -3 V bias.

In order to better understand the performance of the photodiodes we have also performed bit error ratio (BER) measurements at bit rate between 20 and 40 Gb/s . A 1550 nm optical source is intensity modulated by a Mach-Zehnder modulator with a PRBS $2^{31}-1$ pattern and coupled into the receiver input facet. The RF electrical signal generated from the PIN photodetector reverse biased at -3 V is analyzed in terms of BER and eye-diagram respectively by a BER tester and an oscilloscope. Fig. 3b reports the measured bit error rate versus the received

optical power and the corresponding NRZ-OOK eye diagrams with received power to the PD of 5 dBm (assuming 8 dB coupling loss). The sensitivity for a bit rate of 25 Gb/s is about 3.5 dBm (BER=1E-9). The low sensitivity is attributed to a small ($<1\mu\text{m}$) overlap of the p-metal layer and n-contact, causing a short that results in lower responsivity and a high dark current.

3. Delay Interferometer Characterization

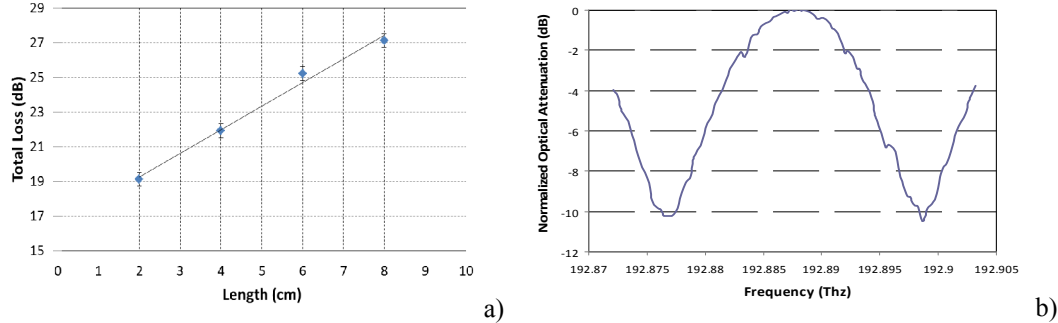


Fig. 4 a) Attenuation measurements by cut back method of the spiral waveguides. b) Spectral response of the delay interferometer filter. Optical output power vs frequency

The DQPSK receiver is able to convert the differential phase modulation in intensity modulation for both quadratures of the signal carrier using two delay interferometers (DI). For each DI a 1x2 Multimode interference (MMI) based splitter splits the light into a waveguide and a spiral waveguide delay-line with a length of 3.8 mm equivalent to a 40-ps time delay (1 period symbol) respect to the other waveguide. The two waveguides are then combined in 2x2 combiner and received by the balanced photodetector. In order to fully characterize the DI, spiral waveguides of different lengths (2- 8 cm) was included in the mask layout for the measurement of the spiral waveguide attenuation by the cut-back method. Two lensed fibers are used to couple light (1550 nm) in and out of the optical spiral waveguides using a top-view infrared camera for fiber alignment. The Fig.4a shows the total measured loss (waveguide attenuation + coupling loss) versus the length of the waveguides. The waveguide attenuation is 1.36 dB/cm and the coupling loss at the input and the output facets is 8.25 dB. In order to characterize the delay interferometer filter, the light coupled at the input of the DQPSK demodulator was collected at the output on the opposite facet of the chip. As in the previous measurement, light from a tunable semiconductor laser is coupled into the SOI waveguide by a single-mode lensed fiber, on the opposite facet of the chip is collected by a second lensed fiber and the power is measured by an optical power meter. The polarization at the input of the demodulator was optimized using a polarization controller in order to have input TE polarization. A frequency sweep of the tunable laser around 1550 nm gives the typical square cosine spectral response of the delay interferometer as shown in Fig.4b. The DI has a period of approximately 22 GHz. In particular for the two delay interferometers on the same receiver was measured respectively a delay time of 45.4 ps and 44.6 ps.

4. Conclusions

Preliminary DQPSK receiver characterization was performed on the stand-alone single photodetector test structures verifying a PD operation at 25 Gb/s, and on the DI that shows a delay time around 44 ps. Demonstration of this device as a receiver with DQPSK data will be presented.

This research was supported by a grant from Rockwell Collins.

5. References

- [1] P.J. Winzer, R.-J. Essiambre, Advanced Optical Modulation formats, Proceedings of IEEE , Vol. 94, Issue 5, pp. 952-985 (2006)
- [2] P. J. Winzer, G. Raybon, H. Song, A. Adamiecki, S. Corteselli, A. H. Gnauck, D. A. Fishman, C. R. Doerr, S. Chandrasekhar, L. L. Buhl, T. J. Xia, G. Wellbrock, W. Lee, B. Basch, T. Kawanishi, K. Higuma, and Y. Painchaud, 100-Gb/s DQPSK Transmission: From Laboratory Experiments to Field Trials, IEEE Journal of Lightwave Technology, Vol. 26, Issue 20, pp. 3388-3402 (2008)
- [3] C. van Trigt, "Visual system-response functions and estimating reflectance," JOSA A **14**, 741-755 (1997).
- [4] Winzer, P. J., Essiambre, R.-J., "Advanced Modulation Formats for High-Capacity Optical Transport Networks," Journal of Lightwave Technology, , vol.24, no.12, pp.4711-4728, Dec. 2006
- [5] Doerr, C.R.; Long Chen, "Monolithic PDM-DQPSK receiver in silicon," Optical Communication (ECOC), 2010 36th European Conference and Exhibition on , vol. , no. , pp.1-3, 19-23 Sept. 2010
- [6] H. Park, A. W. Fang, D. Liang, Y.-H. Kuo, H.-H. Chang, B. R. Koch, H.-W. Chen, M. N. Sysak, R. Jones, and J. E. Bowers, "Photonic Integration on the Hybrid Silicon Evanescent Device Platform ", Advances in Optical Technologies, Article ID 682978, 2008
- [7] H. - H. Chang, Y. - H. Kuo, R. Jones, A. Barkai, J. E. Bowers, "Integrated Hybrid Silicon Triplexer", Optics Express 18, N. 23, pp. 23891 - 23993 (2010)